Coupled ac photocurrent and photothermal reflectance response theory of semiconducting *p-n* junctions. I

Andreas Mandelis
Photoacoustic and Photothermal Sciences Laboratory, Department of Mechanical Engineering and Ontario Laser and Lightwave Research Center, University of Toronto, Toronto, Ontario M5S 1A4, Canada

(Received 12 December 1988; accepted for publication 8 August 1989)

A formalism involving the ac photocurrent and photothermal reflectance (PTR) spectroscopic response of a semiconducting *p-n* junction device is presented. The differential equations for the photovoltaic and PTR signals are solved explicitly and special limits of use in experimental applications [J. Appl. Phys. **66**, 5584 (1989), part II] are considered. The dependence of the photocurrent and PTR signal modulation frequency response on electronic transport parameters is identified and the suitability of ac PTR as a noncontact diagnostic technique is assessed in comparison with the more conventional ac photocurrent method.

I. INTRODUCTION

ac photovoltage measurements have long been used successfully to monitor electronic transport properties in semiconducting devices in general,[1] and in *p-n* junctions in particular.[2,3] Typical measurements are essentially nondestructive, however, they require electrode attachments to the *p-n* junction wafer in order to monitor photovoltage and/or photocurrent.

The recent emergence of ac photothermal reflection (PTR) techniques[4] and their successful application to the measurement of substrate wafer processing paramters,[5] free-carrier plasma densities,[6] and microelectronic device imaging,[7] has raised the possibility of performing nondestructive, noncontact studies of electronic transport parameters at the device level. In order to assess the usefulness of the ac PTR technique in achieving that goal in the case of a basic building-block device such as a *p-n* junction, one must compare the potential of ac PTR with that of the conventional ac photovoltage method through mathematical modeling.

To the best of the author's knowledge, and perhaps surprisingly so, there appears to exist no rigorous theoretical analysis of the ac photocurrent method that would cover the entire set of optical, electronic, and geometric parameters involved in the operation of a conventional *p-n* junction device. Given that the development of an appropriate rigorous ac PTR theory of electronic transport in such a device requires extensive results from the formulation of the ac photovoltaic problem, this work presents a joint analysis of the coupled ac photovoltaic and PTR signal generation problems. It is worthwhile noting that the ac photovoltaic model can be utilized independently for the interpretation of conventional experimental photocurrent results, as shown in part II of this work.[8]

II. ac *p-n* JUNCTION PHOTOVOLTAIC THEORY

A. General formulation

In formulating the theory, great simplification occurs in the case of one-dimensional analysis. For a typical *p-n* junction device, such as a Si solar cell, junction depths are of the order of 1 μm or less[9] and therefore one-dimensional analysis along the depth coordinate can be used for a typical photoexciting optical source beamwidth of a few micrometers. This type of source is experimentally represented by a focused laser beam, and was used in the experiments reported in part II. Thus, in what follows we have used a one-dimensional analysis as a satisfactory approximation to both photovoltaic and PTR problems.

The geometry adopted is that of an abrupt *p-n* junction fabricated on an *n*-type substrate wafer by diffusing a *p*-type impurity so as to form a thin *p*-type surface layer. Figure 1 shows the situation in which the finite width of the depletion region at the junction has been neglected. This is a good approximation under the usual device operation conditions[10] and further simplifies the analysis while retaining the basic physics of the problem. Under monochromatic light excitation of the *p-n* junction, the flux of photons penetrating depth x in the device is given by

$$N(x,t) = N_0 \exp[-\beta(\lambda)(x+d)]H(t)\,, \tag{1}$$

where $H(t)$ is a function determining the time dependence of the incident radiation, d is the junction depth, and $\beta(\lambda)$ is the optical absorption coefficient of the photoexcited material at the excitation wavelength λ. $\beta(\lambda)$ is usually a function of doping concentration in a given semiconducting device. N_0 is the surface photon flux $F_0(\lambda)$ corrected for the reflectivity $R(\lambda)$:

$$N_0(\lambda) = F_0(\lambda)[1 - R(\lambda)]\,. \tag{2}$$

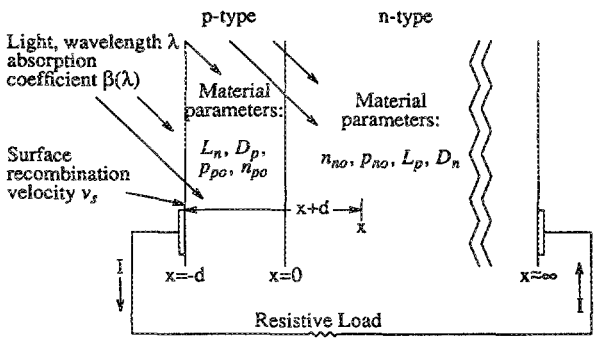

FIG. 1. Cross-sectional view of a *p-n* junction photovoltaic device excited by monochromatic light of frequency $f = \omega/2\pi$.

 0021-8979/89/235572-12$02.40

The time-dependent photogenerated rate of electron-hole pair population at depth x is

$$G(x,t) = -\frac{\partial}{\partial x}N(x,t)$$
$$= \beta(\lambda)N_0(\lambda)H(t)\exp[-\beta(\lambda)(x+d)]\,. \quad (3)$$

Equation (3) plays the role of placing an excess carrier source at the junction depth. These carriers are subsequently separated according to their sign by the built-in electric field and appear as minority carriers on either side of the junction. Charge transport occurs according to the continuity equations:

$$\frac{\partial^2(\Delta n_p)}{\partial x^2} - \frac{\Delta n_p}{L_n^2} - \frac{1}{D_n}\frac{\partial}{\partial t}(\Delta n_p) = -\frac{1}{D_n}G(x,t),$$
$$p \text{ side: } -d \ll x < 0 \quad (4a)$$

and

$$\frac{\partial^2(\Delta p_n)}{\partial x^2} - \frac{\Delta p_n}{L_p^2} - \frac{1}{D_p}\frac{\partial}{\partial t}(\Delta p_n) = -\frac{1}{D_p}G(x,t),$$
$$n \text{ side: } -x > 0\,. \quad (4b)$$

Equations (4) assume that no external applied electric fields exist across the device. L_i and D_i are the minority-carrier diffusion length and diffusion coefficient, respectively ($i = n,p$). Δn_p (Δp_n) is the minority electron (hole) excess density on the $p(n)$ side following illumination. The validity of Eqs. (4) is subject to the following constraints:

$$n_{p_0} \ll p_{p_0}\,, \quad p_{n_0} \ll n_{n_0}\,, \quad (5)$$
$$n_p(x,t) - n_{p_0} \equiv \Delta n_p(x,t) \ll p_{p_0}\,,$$
$$p_n(x,t) - p_{n_0} \equiv \Delta p_n(x,t) \ll n_{n_0}\,. \quad (6)$$

The quantities n_{p_0} (p_{n_0}) and n_{n_0} (p_{p_0}) represent equilibrium minority electron (hole) and majority electron (hole) densities on the $p(n)$ side, respectively. Under harmonic intensity modulation of the optical exciting beam at angular frequency $\omega = 2\pi f$, the excess carrier density time dependence can be described as

$$\Delta n_p(x,t) \equiv n_p(x,t) - n_{p_0} = \Delta n(x)e^{i\omega t}\,, \quad (7a)$$
$$\Delta p_n(x,t) \equiv p_n(x,t) - p_{n_0} = \Delta p(x)e^{i\omega t}\,. \quad (7b)$$

Under harmonic intensity modulation, the time-dependent function in Eq. (3) can be written as

$$H(t) = \tfrac{1}{2}(1 + e^{i\omega t})\,,$$

so that the ac components of Eqs. (4) can be written in the form

$$\frac{d^2}{dx^2}[\Delta n(x)] - \frac{\Delta n(x)}{L_{\omega n}^2} = -\left(\frac{\beta N_0}{2D_n}\right)\exp[-\beta(x+d)]\,,$$
$$-d \ll x < 0\,, \quad (8a)$$

$$\frac{d^2}{dx^2}[\Delta p(x)] - \frac{\Delta p(x)}{L_{\omega p}^2} = -\left(\frac{\beta N_0}{2D_p}\right)\exp[-\beta(x+d)]\,,$$
$$x > 0\,. \quad (8b)$$

In Eqs. (8) the quantities $L_{\omega j}$ have been defined as complex frequency-dependent carrier diffusion lengths ($j = n,p$)

$$L_{\omega j} \equiv L_j/\sqrt{1 + i\omega\tau_j}\,, \quad (9)$$

where τ_j is the minority-carrier lifetime

$$\tau_j = L_j^2/D_j\,. \quad (10)$$

ac photoexcitation of the p-n junction amounts to forward biasing, with the value of the potential barrier modulated at frequency $f = \omega/2\pi$. The barrier height can be written (Fig. 2)

$$V(t) = \phi_0 - V_p(t)\,, \quad (11)$$

where

$$V_p(t) \equiv V_0 e^{i\omega t}\,. \quad (12)$$

Under the abrupt junction and infinitesimal depletion-width approximation, the excess minority-carrier densities on either side of the junction boundary at $x = 0$ under illumination can be given in terms of the equilibrium densities[10]

$$\frac{n_p(0,t)}{n_{n_0}} = \frac{p_n(0,t)}{p_{p_0}} = \exp\left(-\frac{q[\phi_0 - V_p(t)]}{k_B T}\right). \quad (13)$$

In the small signal approximation

$$V_0 \ll k_B T/q\,, \quad (14)$$

the exponential term may be expanded and the first term linear in ω retained:

$$\exp\{-q[\phi_0 - V_p(t)]/k_B T\}$$
$$= \exp(-q\phi_0/k_B T)\exp(qV_0 e^{i\omega t}/k_B T)$$
$$\approx \exp(-q\phi_0/k_B T)[1 + (qV_0/k_B T)e^{i\omega t}]\,. \quad (15)$$

Using

$$n_{p_0} = n_{n_0}\exp(-q\phi_0/k_B T)\,, \quad (16a)$$

$$p_{n_0} = p_{p_0}\exp(-q\phi_0/k_B T)\,, \quad (16b)$$

Eqs. (13), (15), and (16) yield the relations

$$\frac{\Delta n(0)}{n_{p_0}} = \frac{\Delta p(0)}{p_{n_0}} \approx \frac{qV_0}{k_B T}\,, \quad (17)$$

which are the boundary conditions at $x = 0$ under the linearizing assumption of a small ac signal component. In the case of an incident high-intensity laser beam such that the maximum photovoltage V_0 does not satisfy condition (14), the present formalism predicts the appearance of nonlinear terms in the photovoltaic response of the device. Neglecting

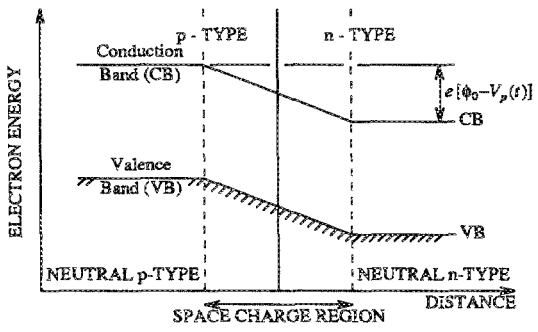

FIG. 2. Energy-band diagram of p-n junction illuminated under ac photoexcitation of modulation frequency $f = \omega/2\pi$. ϕ_0 is the contact potential; $V_p(t)$ is the time-dependent photovoltage.

any such terms and assuming a semi-infinite n-type substrate (Fig. 1), two more boundary conditions must be satisfied:

$$\Delta p(\infty) = 0 \tag{18}$$

and

$$D_n \frac{d}{dx}[\Delta n(x)]_{x=-d} = v_s \Delta n(-d), \tag{19}$$

where v_s is the surface recombination velocity.

The solution of Eqs. (8) yields the expressions

$$\Delta n(x) = A\cosh(x/L_{\omega n}) + B\sinh(x/L_{\omega n}) + \frac{\beta N_0 L_{\omega n}^2}{2D_n(1-\beta^2 L_{\omega n}^2)} e^{-\beta(x+d)}, \quad -d \leqslant x < 0, \tag{20a}$$

$$\Delta p(x) = Ce^{x/L_{\omega p}} + De^{-x/L_{\omega p}} + \frac{\beta N_0 L_{\omega p}^2}{2D_p(1-\beta^2 L_{\omega p}^2)} e^{-\beta(x+d)}, \quad x > 0. \tag{20b}$$

The constants A, B, C, and D can be determined from boundary conditions (17)–(19) and are given as follows:

$$A = n_{p_0}\left(\frac{qV_0}{k_B T}\right) - \frac{\beta N_0 L_{\omega n}^2}{2D_n(1-\beta^2 L_{\omega n}^2)} e^{-\beta d}, \tag{21}$$

$$B = A\left(\frac{v_s\cosh(d/L_{\omega n}) + (D_n/L_{\omega n})\sinh(d/L_{\omega n})}{(D_n/L_{\omega n})\cosh(d/L_{\omega n}) + v_s\sinh(d/L_{\omega n})}\right) + \frac{\beta N_0 L_{\omega n}^2}{2D_n(1-\beta^2 L_{\omega n}^2)} \times\left(\frac{v_s + \beta D_n}{(D_n/L_{\omega n})\cosh(d/L_{\omega n}) + v_s\sinh(d/L_{\omega n})}\right), \tag{22}$$

$$C = 0, \tag{23}$$

$$D = p_{n_0}\left(\frac{qV_0}{k_B T}\right) - \frac{\beta N_0 L_{\omega p}^2}{2D_p(1-\beta^2 L_{\omega p}^2)} e^{-\beta d}. \tag{24}$$

Neglecting any thermal generation or recombination of carriers within the depletion layer can be justified in typical device geometries where the width of that layer is quite small compared to carrier diffusion lengths. Under this simplification the junction current density may be calculated by evaluating the diffusion currents of minority carriers at $x = 0$, which represents both the depletion layer boundaries in this model:

$$J(0) = q\left(D_n \frac{d}{dx}\Delta n(x) - D_p \frac{d}{dx}\Delta p(x)\right)_{x=0}. \tag{25}$$

In terms of components, the current density can be separated into functions dependent on, and independent of, the junction barrier potential V_0, respectively:

$$J(0) = J_0(qV_0/k_B T) - J_G. \tag{26}$$

In Eq. (26) J_0 is the saturation current density, which is a function of the geometry and fabrication parameters of the junction. Furthermore, it is independent of the optical intensity. Since J_0 does not represent a photocurrent in response to the incident optical flux, it will not be considered any further in this work. The term J_G represents the generation current and is proportional to the illumination intensity

$$I(h\nu) = N_0 h\nu \quad (\mathrm{W/cm^2}) \tag{27}$$

via its dependence on the incident photon flux N_0. J_G is independent of the junction photopotential V_0 and is a measure of the excess photogenerated electron-hole pairs that are successful in diffusing to the junction before recombining. Therefore, J_G is the only component related to the experimentally observed ac photocurrent and will be exclusively considered in the remainder of this work. From Eqs. (20)–(26) the general expression for the ac photocurrent density can be written in complex form as follows:

$$J_G = \frac{1}{2} q\beta N_0\left\{\frac{L_{\omega p}^2}{1-b^2 L_{\omega p}^2}\left(\frac{1}{L_{\omega p}} - \beta\right)e^{-\beta d} + \frac{L_{\omega n}^2}{1-\beta^2 L_{\omega n}^2} \times\left[\frac{1}{L_{\omega n}}\left(\frac{[v_s\cosh(d/L_{\omega n}) + (D_n/L_{\omega n})\sinh(d/L_{\omega n})]e^{-\beta d} - (v_s + \beta D_n)}{(D_n/L_{\omega n})\cosh(d/L_{\omega n}) + v_s\sinh(d/L_{\omega n})}\right) + \beta e^{-\beta d}\right]\right\}. \tag{28}$$

Equation (28) is the modulation frequency-dependent extension of the dc generation current density expression derived earlier[10] with a sign correction in front of the last term. In the limit of $\omega = 0$, Eq. (9) shows that $L_{\omega j} = L_j$ and Eq. (28) becomes identical to the (corrected) Eq. (15.1-17) of Ref. 10.

For direct experimental comparison, the most convenient representation of the photovoltaic current expression is in terms of polar coordinates, which yield amplitude and phase channel information. Appendix A lists the various complex-valued functions encountered in Eq. (28) in polar coordinate representation. Using those definitions, the amplitude $|J_G|$ and phase Θ_G of the photocurrent signal can be written in the form

$$|J_G| = (X_3^2 + Y_3^2)^{1/2}, \tag{29}$$

$$\Theta_G = \tan^{-1}(Y_3/X_3), \tag{30}$$

where X_3 and Y_3 are defined in Appendix A.

B. Special cases

1. Low-frequency limit

At low light intensity modulation frequencies, such that $\omega\tau_n \ll 1$, $\omega\tau_p \ll 1$, the following approximations to the general theory can be made (see Appendix A):

$$|R_n| \approx |R_p| \approx 1, \tag{31}$$

$$C_n \approx d/L_n, \quad S_n \approx 0, \tag{32}$$

$$|J_1| \approx X_1 \approx v_s \cosh\frac{d}{L_n} + \frac{D_n}{L_n}\sinh\frac{d}{L_n}, \quad \Psi_1 \approx 0, \tag{33}$$

$$|J_2| \approx X_2 \approx \frac{D_n}{L_n}\cosh\frac{d}{L_n} + v_s \sinh\frac{d}{L_n}, \quad \Psi_2 \approx 0, \tag{34}$$

$$|Z_1| \approx |1-(\beta L_n)^2|, \quad \phi_1 \approx 0, \tag{35}$$

$$|Z_2| \approx |1-(\beta L_p)^2|, \quad \phi_2 \approx 0. \tag{36}$$

The signal is independent of modulation frequency, because all carrier transport is fast compared to optical excitation periods; therefore, the photocurrent becomes independent of the observation time (one modulation period). Under these conditions, two important cases may be identified.

(i) $v_s \to 0$:

In this limit the photovoltaic signal becomes

$$|J_G| \approx X_3 \approx \frac{1}{2} q\beta N_0 \left\{ \left(\frac{L_p}{1+\beta L_p}\right) e^{-\beta d} + \frac{L_n}{|1-(\beta L_n)^2|} \times \left[\left(\beta L_n + \tanh\frac{d}{L_n}\right) e^{-\beta d} - \beta L_n \operatorname{sech}\frac{d}{L_n} \right] \right\}, \tag{37}$$

$$\Theta_G \approx 0.$$

In the optically opaque case a further simplification occurs upon setting

$$\exp(-\beta d) \approx 0. \tag{38a}$$

Then, one obtains

$$|J_G| \approx \frac{1}{2} qN_0 \left(\frac{(\beta L_n)^2}{|1-(\beta L_n)^2|}\right) \operatorname{sech}\frac{d}{L_n} \approx \frac{1}{2} qN_0 \operatorname{sech}\frac{d}{L_n}. \tag{39}$$

The photovoltaic signal is optically saturated, i.e., independent of β, provided that $\beta L_n \gg 1$, as expected. In the optically transparent limit,

$$\exp(-\beta d) \approx 1, \tag{38b}$$

so that

$$|J_G| \approx \frac{1}{2} q\beta N_0 \left[\frac{L_p}{1+\beta L_p} + \frac{L_n}{|1-(\beta L_n)^2|} \times \left(\beta L_n + \tanh\frac{d}{L_n} - \beta L_n \operatorname{sech}\frac{d}{L_n}\right) \right]. \tag{40}$$

Upon making the realistic assumption[9] that $d/L_n \ll 1$, Eq. (40) reduces to

$$|J_G| \approx \tfrac{1}{2} qN_0 [\beta L_p/(1+\beta L_p)]. \tag{41}$$

Equation (41) is identical to the expression for the photocurrent presented without derivation by Munakata *et al.*[11] in the limit of low frequencies and for a p-n junction fabricated on a p-type Si wafer, rather than the n-type substrate assumed in this model. The complex extension of Eq. (41) can be readily obtained by substituting $L_{\omega p}$ for L_p. The linear dependence of $|J_G|$ on β at low optical absorption coefficients is due to the fact that the optical penetration depth of the photon beam β^{-1} becomes much longer than the carrier diffusion length and thus the integrated absorption over one diffusion length thickness becomes proportional to the amount of light absorbed, i.e., scales linearly with β. This behavior has also been observed previously.[11]

(ii) $v_s \to \infty$:

In this limit the photovoltaic signal becomes

$$|J_G| \approx X_4 \approx \frac{1}{2} q\beta N_0 \left\{ \left(\frac{L_p}{1+\beta L_p}\right) e^{-\beta d} + \frac{L_n}{|1-(\beta L_n)^2|} \times \left[\left(\beta L_n + \coth\frac{d}{L_n}\right) e^{-\beta d} - \operatorname{csch}\frac{d}{L_n} \right] \right\}, \tag{42}$$

$$\Theta_G \approx 0.$$

For both very low and very high v_s, the phase of the signal remains constant at 0° due to the fast transport response of the device, which is in-phase with the modulated optical excitation. In the optically opaque regime, the signal simplifies to

$$|J_G| \approx \tfrac{1}{2} qN_0 \operatorname{csch}(d/L_n)/\beta L_n, \tag{43}$$

i.e., a monotonic decrease with β, provided that $\beta L_n \gg 1$, due to the fact that $\beta d > 1$ also, so that the p-type region becomes optically opaque and photogenerated minority carriers lie closer to the device surface, where they cease to contribute to the photocurrent generation as they are swept out of the circuit at high recombination velocities (see part II).

2. High-frequency limit

In this case $\omega\tau_n \gg 1$, $\omega\tau_p \gg 1$. Appendix A gives the approximate values

$$|R_j| \approx \omega\tau_j, \quad \phi_j \approx \pi/2 \quad (j = n, p), \tag{44}$$

$$C_n \approx S_n \approx d/\mu_n(\omega), \tag{45}$$

where

$$\mu_j(\omega) \equiv (2D_j/\omega)^{1/2}, \quad j = n, p \tag{46}$$

is the electron ($j = n$) or hole ($j = p$) ac diffusion length associated with the minority-carrier diffusional wave on either side of the junction.

(i) $v_s \to 0$:

In this limit

$$|J_1| \approx \{\omega D_n [\sinh^2(d/\mu_n) + \sin^2(d/\mu_n)]\}^{1/2}, \tag{47}$$

$$\Psi_1 \approx \tan^{-1}\left(\frac{\sinh(d/\mu_n)\cos(d/\mu_n) + \cosh(d/\mu_n)\sin(d/\mu_n)}{\sinh(d/\mu_n)\cos(d/\mu_n) - \cosh(d/\mu_n)\sin(d/\mu_n)}\right), \tag{48}$$

and

$$|J_2| = \{\omega D_n [\sinh^2(d/\mu_n) + \cos^2(d/\mu_n)]\}^{1/2}, \tag{49}$$

$$\Psi_2 = \tan^{-1}\left(\frac{\cosh(d/\mu_n)\cos(d/\mu_n) + \sinh(d/\mu_n)\sin(d/\mu_n)}{\cosh(d/\mu_n)\cos(d/\mu_n) - \sinh(d/\mu_n)\sin(d/\mu_n)}\right). \tag{50}$$

Furthermore,

$$|Z_1| \approx [1 + (\beta\mu_n)^4]^{1/2}, \quad \phi_1 \approx \tan^{-1}[(\beta\mu_n)^2/2], \tag{51}$$

$$|Z_2| \approx [1 + (\beta\mu_p)^4]^{1/2}, \quad \phi^2 \approx \tan^{-1}[(\beta\mu_p)^2/2]. \tag{52}$$

For very high frequencies, such that

$$\omega \gg \max(2D_n/d^2, 2D_n\beta^2, 2D_p\beta^2), \tag{53}$$

we can write

$$d/\mu_n(\omega) \gg 1; \quad \beta\mu_n(\omega), \quad \beta\mu_p(\omega) \ll 1.$$

Under these conditions, and in the optically opaque limit, $\exp(-\beta d) \approx 0$, the photocurrent signal becomes

$$|J_G| \approx \tfrac{1}{2} qN_0[\beta\mu_n(\omega)]^2 \exp[-d/\mu_n(\omega)], \tag{54}$$

$$\Theta_G \approx \frac{\pi}{4} + \tan^{-1}\left(\frac{\cos(d/\mu_n) + \sin(d/\mu_n)}{\cos(d/\mu_n) - \sin(d/\mu_n)}\right). \tag{55}$$

The ac photocurrent amplitude decays with increasing ω as a result of the modulation frequency becoming comparable to, or higher than, the recombination rate (the inverse lifetime) of the photogenerated carriers: this effect tends to decrease the observed photocurrent due to incomplete collection of carriers at the junction and subsequent diffusion to the measuring electrode location at $x = -d$. The functional form of this decrease is exponential with decreasing $\mu_n(\omega)$, as expected from a heavily damped diffusional wave, with a mild preexponential frequency dependence on ω^{-1} as well. The nonzero phase shift Θ_G indicates the diffusional delay due to the inability of the photogenerated carriers to respond fast enough to the optical excitation.

(ii) $v_s \to \infty$:

In this limit

$$|J_1| \approx v_s[\sinh^2(d/\mu_n) + \cos^2(d/\mu_n)]^{1/2}, \tag{56}$$

$$\Psi_1 \approx \tan^{-1}[\tan(d/\mu_n)\tanh(d/\mu_n)]. \tag{57}$$

Also

$$|J_2| \approx v_s[\sinh^2(d/\mu_n) + \sin^2(d/\mu_n)]^{1/2}, \tag{58}$$

with

$$\Psi_2 \approx \tan^{-1}[\tan(d/\mu_n)\coth(d/\mu_n)]. \tag{59}$$

At very high frequencies where condition (53) is valid, and in the optically opaque limit, the expression for the photocurrent signal becomes

$$|J_G| \approx (\sqrt{2}/2)qN_0[\beta\mu_n(\omega)]\exp[-d/\mu_n(\omega)], \tag{60}$$

$$\Theta_G \approx (\pi/4) + d/\mu_n(\omega). \tag{61}$$

The causes of the ac photocurrent amplitude decay and phase lag are similar to those discussed above in the $v_s = 0$ case. The particular functional dependencies here involve, again, an exponential amplitude decay with decreasing $\mu_n(\omega)$, along with a $\omega^{-1/2}$ preexponential dependence, whereas the phase lag increases linearly with $\omega^{1/2}$. Both of these mild fractional power dependencies are due to the frequency-dependent carrier diffusion length $L_{\omega n}$, Eq. (9), becoming the limiting quantity in the device response.

III. ac *p-n* JUNCTION PHOTOTHERMAL REFLECTANCE THEORY

A. General formulation: The thermal wave problem

The PTR technique hinges on the fact that the sample surface reflectivity is a function of temperature.[12] In the case of electronically active materials, such as semiconductors, super-band-gap optical excitation results in the generation of free electron-hole pairs within a thin region below the surface, which also intersects the junction in a photovoltaic device. The excess photocarrier density at the surface also contributes a component to the reflectivity.[6] In its most general form, optical heating of a semiconductor surface using an intensity-modulated laser source results in a fractional change ΔR of the unperturbed surface reflectance R_0 given by

$$\left.\frac{\Delta R}{R_0}\right|_{\text{surf}} = \frac{1}{R_0}\left(\frac{\partial R}{\partial T}\right)\Delta T_{\text{surf}} + \frac{1}{R_0}\left(\frac{\partial R}{\partial n}\right)\Delta n_{\text{surf}}. \tag{62}$$

In Eq. (62), ΔT_{surf} is the surface temperature excursion following optical heating, ΔN_{surf} is the photoexcited free-carrier density at the surface, and $\partial R/\partial T$, $\partial R/\partial n$ are material parameters assumed constant. For pure Si,[13] $(\partial R/\partial T)/R_0 \equiv a \approx 1.5\times 10^{-4}/^{\circ}\text{C}$, and[6] $(\partial R/\partial n)/R_0 \equiv b \approx -10^{-22}$ cm^3. Equation (62) may then be written as

$$\left.\frac{\Delta R}{R_0}\right|_{\text{surf},\omega} = a\Delta T(-d,\omega) + b\Delta n(-d,\omega). \tag{63}$$

Opsal and Rosencwaig have shown[6] that, for the case of optical excitation of a pure Si substrate, both terms on the right-hand side of Eq. (63) are of the same order, albeit of opposite signs, and are both important in determining the thermoreflectance response of pure Si. In their case $\Delta n = n_n - n_{n_0}$, i.e., Δn is the excess photoexcited plasma density in intrinsic or doped substrates: $\Delta n \approx 10^{18}$ cm^{-3}. For the photovoltaic *p-n* junction device of Fig. 1, however, the second term on the right-hand side of Eq. (62) consists of the free minority-carrier density increase due to the presence of the optical field. It should be recalled that $\Delta n(x)$ is the magnitude of the excess minority electron density on the *p* side and is given by Eq. (7a). As such $\Delta n \lesssim 10^{10}$ cm^{-3}, or $\Delta n(-d,\omega) \ll p_{p_0}$, the periodic surface equilibrium majority hole density. Therefore, it is clear that for a *p-n* junction device the second term on the right-hand side of Eq. (63) is much less significant than the first term and one can write

$$\left.\frac{\Delta R}{R_0}\right|_{\text{surf},\omega} \approx a\Delta T(-d,\omega). \tag{63'}$$

For small departures from the background temperature T_0, optical heating of the device can be described by

$$\alpha\frac{\partial^2(\Delta T_p)}{\partial x^2}+\left(\frac{\beta N_0\Delta E}{\rho c}\right)e^{-\beta(x+d)}+\frac{E_g}{\tau_n\rho c}(\Delta n_p)$$
$$=\frac{\partial}{\partial t}(\Delta T_p),\quad p\text{ side: }\ -d\leqslant x<0 \tag{64a}$$

and

$$\alpha\frac{\partial^2(\Delta T_n)}{\partial x^2}+\left(\frac{\beta N_0\Delta E}{\rho c}\right)e^{-\beta(x+d)}+\frac{E_g}{\tau_p\rho c}(\Delta p_n)$$
$$=\frac{\partial}{\partial t}(\Delta T_n),\quad n\text{ side: }\ x>0. \tag{64b}$$

In Eqs. (64) $\Delta T_p(\Delta T_n)$ is the temperature excursion from T_0 in the p (n) side; E_g is the band-gap energy of the semiconductor homojunction material; $\Delta E=h\nu-E_g$ is the thermalization energy that results from optically excited carrier relaxation following absorption of photons with energy higher than E_g; and α, ρ, and c are the material thermal diffusivity, density, and specific heat, respectively. These governing equations are simplified versions of a more complete set, in which the heat generation rate is given by[14]

$$G_H(x,t)=[h\nu N_0(\lambda)\beta_{\text{FC}}\,e^{-\beta(x+d)}$$
$$+(h\nu-\eta_Q E_R)N_0(\lambda)\beta_1 e^{-\beta(x+d)}$$
$$+(E_R/\tau_{\text{NR}})\Delta n]H(t), \tag{65}$$

where $\beta=\beta_{\text{FC}}+\beta_1$, with β_{FC} representing the free-carrier absorption coefficient and β_1 is the single-photon band-to-band absorption coefficient. Two-photon and higher nonlinear absorption processes can be neglected for low illumination intensities. η_Q is the quantum efficiency for one-photon carrier generation, E_R is the average electron-hole recombination energy, and τ_{NR} is the nonradiative component of the bulk lifetime. It is reasonable to make the following approximations to several parameters in Eq. (65): $E_R\approx E_g$, for small quasiequilibrium values of the average electron (hole) energy above (below) the conduction (valence) band edge; $\tau_{\text{NR}}\approx\tau_p(\tau_n)$, for room-temperature measurements where radiative and photochemical deexcitation channels in the $p(n)$ side of the junction are insignificant; this further implies $\eta_Q\approx 1$; $\beta_{\text{FC}}\ll\beta_1\approx\beta$, for minority-carrier populations much smaller than majority-carrier densities on either side of the p-n junction.

With these approximations,

$$G_{H_p}(x,t)\approx[(\beta N_0\Delta E)e^{-\beta(x+d)}$$
$$+(E_g/\tau_n)\Delta n_p(x)]H(t), \tag{66a}$$
$$G_{H_n}(x,t)\approx[(\beta N_0\Delta E)e^{-\beta(x+d)}$$
$$+(E_g/\tau_p)\Delta p_n(x)]H(t). \tag{66b}$$

Now, under ac optical heating we can define

$$\Delta T_p(x,t)\equiv\Delta T_p(x)e^{i\omega t}, \tag{67a}$$
$$\Delta T_n(x,t)\equiv\Delta T_n(x)e^{i\omega t}, \tag{67b}$$

and, recalling Eqs. (7), the thermal diffusion equations (67) can be written

$$\frac{d^2}{dx^2}[\Delta T_p(x)]-\sigma^2\Delta T_p(x)$$
$$=-\left(\frac{E_g}{2k}\tau_n\right)\left(A\cosh\frac{x}{L_{\omega n}}+B\sinh\frac{x}{L_{\omega n}}\right)$$
$$-\frac{\beta N_0}{2k}\left(\Delta E+\frac{E_g L_{\omega n}^2}{L_n^2(1-\beta^2L_{\omega n}^2)}\right)e^{-\beta(x+d)},$$
$$-d\leqslant x<0, \tag{68a}$$

$$\frac{d^2}{dx^2}[\Delta T_n(x)]-\sigma^2\Delta T_n(x)$$
$$=-\left(\frac{E_g D}{2k\tau_p}\right)e^{-x/L_{\omega p}}-\left(\frac{\beta N_0}{2k}\right)$$
$$\times\left(\Delta E+\frac{E_g L_{\omega p}^2}{L_p^2(1-\beta^2L_{\omega p}^2)}\right)e^{-\beta(x+d)},\quad x>0. \tag{68b}$$

In Eqs. (68) k is the material thermal conductivity ($=\alpha\rho c$); A, B, D were defined in Eqs. (21)–(24); $\sigma\equiv(i\omega/\alpha)^{1/2}$ is the complex thermal diffusion coefficient. The small signal approximation, Eq. (14), was assumed throughout. Solution of Eqs. (68) gives the expressions for the temperature on either side of the junction:

$$\Delta T_p(x)=C_1\cosh[\sigma(x+d)]+C_2\sinh[\sigma(x+d)]$$
$$+\frac{E_g}{k\tau_n(\sigma^2-L_{\omega n}^{-2})}\left(A\cosh\frac{x}{L_{\omega n}}\right.$$
$$\left.+B\sinh\frac{x}{L_{\omega n}}\right)+\frac{\beta N_0}{2k(\sigma^2-\beta^2)}$$
$$\times\left(\Delta E+\frac{E_g L_{\omega n}^2}{L_n^2(1-\beta^2L_{\omega n}^2)}\right)e^{-\beta(x+d)} \tag{69}$$

and

$$\Delta T_n(x)=C_3\,e^{-\sigma(x+d)}+\left(\frac{E_g D}{k\tau_p(\sigma^2-L_{\omega p}^{-2})}\right)e^{-x/L_{\omega p}}$$
$$+\frac{\beta N_0}{2k(\sigma^2-\beta^2)}\left(\Delta E+\frac{E_g L_{\omega p}^2}{L_p^2(1-\beta^2L_{\omega p}^2)}\right)$$
$$\times e^{-\beta(x+d)}. \tag{70}$$

Three boundary conditions must be satisfied for the p-n junction device of Fig. 1, corresponding to the three integration constants C_1–C_3. These include temperature and heat flux continuity at the interface $x=0$:

$$\Delta T_p(0)=\Delta T_n(0), \tag{71}$$
$$\frac{d}{dx}[\Delta T_p(x)]_{x=0}=\frac{d}{dx}[\Delta T_n(x)]_{x=0}. \tag{72}$$

Equation (72) assumes constant thermal conductivity across the space-charge region. The last boundary condition involves the rate of heat generation at the surface[14]:

$$k\frac{d}{dx}[\Delta T_p(x)]_{x=-d}=-v_s^{\text{NR}}\Delta n(-d)E_R, \tag{73}$$

where v_s^{NR} is the part of the total surface recombination ve-

locity due to nonradiative processes. In accord with our previous approximations, and in view of the complete neglect of radiative and photochemical deexcitation channels in this work, we shall set $v_s^{NR} \approx v_s$. Thus Eq. (73) can be written in the approximate form

$$k\frac{d}{dx}[\Delta T_p(x)]_{x=-d} \approx -v_s E_g \Delta n(-d). \tag{74}$$

Now the constants C_1, C_2, C_3 can be determined from Eqs. (71), (72), and (74). Once the expressions for A, B, and D have also been inserted from Eqs. (21)–(24), the complex-valued equation for $\Delta T_p(-d)$ will have the form

$$\Delta T_p(-d) = \Delta T_0(-d)(q\bar{V}_0/k_B T) - \Delta T_G(-d), \tag{75}$$

where $\Delta T_0(-d)$ is independent of the incident photon flux N_0 and $\Delta T_G(-d)$ is the surface temperature excursion related to the photogenerated free-carrier recombination. In line with the photocurrent formalism of Sec. II, only the ΔT_G term will be considered throughout the rest of this work, i.e., the ac temperature term resulting from nonradiative energy release from free minority carriers recombining on the surface of the p-n junction device. Under these conditions, the full complex expression for $\Delta n(-d)$ to be used in Eq. (74) may be given using the N_0-dependent component

$$\Delta n(-d) = \frac{\beta N_0 L_{\omega n}^2}{1-\beta^2 L_{\omega n}^2}\left(\frac{L_{\omega n}^{-1}[\cosh(d/L_{\omega n}) - e^{-\beta d}] - \beta \sinh(d/L_{\omega n})}{(D_n/L_{\omega n})\cosh(d/L_{\omega n}) + v_s \sinh(d/L_{\omega n})}\right). \tag{20a'}$$

Finally, the expression for the complex ac surface temperature can be written after considerable algebraic manipulation:

$$\begin{aligned}\Delta T_G(-d) = \frac{\beta E_g N_0}{2k}\Bigg(&\frac{L_{\omega p}^2 e^{-(\beta+\sigma)d}}{L_p^2(1-\beta^2 L_{\omega p}^2)\sigma}\left(\frac{1}{\sigma + L_{\omega p}^{-1}} - \frac{1}{\sigma+\beta}\right)\\ &+ \frac{L_{\omega n}^2}{L_n^2(1-\beta^2 L_{\omega n}^2)}\Bigg\{\Bigg[\Bigg\{\frac{1}{\sigma^2 - L_{\omega n}^{-2}}\Bigg\{\frac{D_n}{L_{\omega n}}e^{-\beta d} + (v_s + \beta D_n)\sinh\frac{d}{L_{\omega n}}\\ &+ (\sigma L_{\omega n})^{-1}\Bigg[v_s e^{-\beta d} - (v_s + \beta D_n)\left(\cosh\frac{d}{L_{\omega n}} + e^{-\sigma d}\right) - \left(v_s\cosh\frac{d}{L_{\omega n}} + \frac{D_n}{L_{\omega n}}\sinh\frac{d}{L_{\omega n}}\right)e^{-(\beta+\sigma)d}\Bigg]\Bigg\}\\ &+ \left(v_s\frac{\tau_n}{\sigma}\right)\Bigg[\beta D_n \sinh\frac{d}{L_{\omega n}} + \frac{D_n}{L_{\omega n}}\left(e^{-\beta d} - \cosh\frac{d}{L_{\omega n}}\right)\Bigg]\Bigg]\Bigg/\left(\frac{D_n}{L_{\omega n}}\cosh\frac{d}{L_{\omega n}} + v_s\sinh\frac{d}{L_{\omega n}}\right)\Bigg]\\ &- \frac{1}{\sigma}\Bigg[\frac{1}{\sigma+\beta} - \left(\frac{1}{\sigma+\beta} - \frac{1}{\sigma[1-(\sigma L_{\omega n})^{-2}]}\right)e^{-(\beta+\sigma)d}\Bigg]\Bigg\}\Bigg).\end{aligned} \tag{76}$$

Straightforward physical interpretation of Eq. (76) is difficult in the general case, however, amplitude $|\Delta T_G|$ and phase $\Theta_{\Delta T}$ corresponding to experimental data channels may be separated out with the help of Appendix B.

B. Special cases

In this section we shall consider several special cases of the optically opaque limit expressed by Eq. (38a). This condition reflects essential physical constraints of actual p-n junction devices that are coated with antireflection coatings and represents experimental conditions described in part II.[8] When Eq. (38a) is valid, Eq. (B8) simplifies to the following expression:

$$\begin{aligned}X_4 = \frac{\beta E_g N_0}{2k_s|R_n||Z_1|}\Bigg[&\frac{1}{|J_2|}\Bigg(\frac{1}{|Z_3|}\Bigg\{(v_s+\beta D_n)|Z_s|\cos(\phi_n+\phi_1+\phi_3+\psi_2-\phi_s) - \frac{|R_n|^{1/2}}{\sqrt{2}a_t L_n}(v_s+\beta D_n)\\ &\times\Bigg[|Z_c|\cos\left(\frac{\phi_n}{2}+\phi_1+\phi_3+\psi_2+\frac{\pi}{4}-\phi_c\right) + e^{-a_t d}\cos\left(\frac{\phi_n}{2}+\phi_1+\phi_3+\psi_2+a_t d+\frac{\pi}{4}\right)\Bigg]\Bigg\}\\ &- \frac{v_s\tau_n}{\sqrt{2}a_t}\Bigg[\frac{D_n|R_n|^{1/2}}{L_n}|Z_c|\cos\left(\frac{\phi_n}{2}+\phi_1+\psi_2+\frac{\pi}{4}-\phi_c\right) - \beta D_n|Z_s|\cos\left(\phi_n+\phi_1+\psi_2+\frac{\pi}{4}-\phi_2\right)\Bigg]\Bigg)\\ &- \frac{1}{\sqrt{2}a_t|Z_4|}\cos\left(\phi_n+\phi_1+\phi_4+\frac{\pi}{4}\right)\Bigg],\end{aligned} \tag{77}$$

with an analogous expression for Y_4 derived from Eq. (B9).

1. Low-frequency limit

In this special case the approximations Eqs. (31)–(36) hold. In addition, from Appendix B,

$$|Z_3| \approx (4a_t^4 + L_n^{-4})^{1/2}, \quad \phi_3 \approx \tan^{-1}(2a_t^2 L_n^2), \tag{78}$$

$$|Z_4| = [(\beta + a_t)^2 + a_t^2]^{1/2} \approx \beta, \quad \phi_4 \approx 0. \tag{79}$$

In the low-frequency regime $\mu_t \equiv a_t^{-1} \gg L_n$, a thermally thin condition involving the thermal diffusion length $\mu_t(\omega)$ and the minority electron diffusion length in the p region. Equation (78) then becomes

$$|Z_3| \approx L_n^{-2}, \quad \phi_3 \approx 0. \tag{80}$$

Similarly, another thermally thin condition encountered at low frequencies is $\mu_t(\omega) \gg d$, or $a_t d \ll 1$, so that $\exp(-a_t d) \approx 1$. Thus, Eq. (77) further reduces to

$$X_4 \approx \frac{\beta E_g N_0}{2k_s |1-(\beta L_n)^2|} \left(\frac{1}{X_2} \left\{ L_n^2 (v_s + \beta D_n) \times \left[\sinh \frac{d}{L_n} - \left(\frac{1}{2a_t L_n} \right) \left(\cosh \frac{d}{L_n} + 1 \right) \right] - \frac{v_s L_n^2}{2a_t} \left(L_n^{-1} \cosh \frac{d}{L_n} - \beta \sinh \frac{d}{L_n} \right) \right\} - \frac{1}{2\beta a_t} \right), \tag{81}$$

and, analogously,

$$Y_4 \approx \frac{\beta E_g N_0}{2k_s |1-(\beta L_n)^2|} \left\{ \frac{1}{X_2} \left[\frac{L_n (v_s + \beta D_n)}{2a_t} \times \left(\cosh \frac{d}{L_n} + 1 \right) + \frac{v_s L_n^2}{2a_t} \times \left(L_n^{-1} \cosh \frac{d}{L_n} - \beta \sinh \frac{d}{L_n} \right) \right] + \frac{1}{2\beta a_t} \right\}, \tag{82}$$

where X_2 is given by Eq. (34). In terms of v_s limits, the following cases may be identified.

(i) $v_s \to 0$:

The real and imaginary components of the temperature-dependent ac PTR signal become

$$X_4 \approx \frac{\beta E_g N_0}{2k |1-(\beta L_n)^2|} \left\{ \beta L_n^3 \left[\tanh \frac{d}{L_n} - \frac{1}{2a_t L_n} \left(1 + \operatorname{sech} \frac{d}{L_n} \right) \right] \right\} \tag{83}$$

and

$$Y_4 \approx \frac{E_g N_0 (\beta L_n)^2}{4k |1-(\beta L_n)^2| a_t} \left[1 + \operatorname{sech}(d/L_n) \right]. \tag{84}$$

In the optically opaque situation where $\mu_\beta \equiv \beta^{-1} \ll d$, we also expect $\mu_\beta \ll L_n$ as a reasonable approximation, since usually $d < L_n$ in p-n junction devices.[9] Under this assumption, Eqs. (83) and (84) can be combined to yield

$$|\Delta T_G| \approx \frac{E_g N_0}{\sqrt{2} k a_t(\omega)} \left(1 + \operatorname{sech} \frac{d}{L_n} \right), \quad \Theta_{\Delta T} \approx -\frac{\pi}{4}. \tag{85}$$

The surface temperature dependence of the ac PTR signal is independent of β and decreases with modulation frequency as $f^{-1/2}$ due to the domination of the signal by the thermal diffusion length $\mu_t(\omega) = a_t^{-1}$ at low frequencies. The ac temperature decreases with increasing modulation frequency, as the optical energy converted to heat decreases with decreasing modulation period. Comparison of Eqs. (39) and (85) shows that both photocurrent and PTR temperature component signals contain similar information about d/L_n, with the latter exhibiting an additional thermal diffusion length factor, as expected.

(ii) $v_s \to \infty$:

In this limit the PTR signal gives

$$X_4 = \frac{\beta E_g N_0}{2k |1-(\beta L_n)^2|} \times \left[1 - \frac{1}{2a_t L_n} \left(2 \coth \frac{d}{L_n} + \operatorname{csch} \frac{d}{L_n} - \beta L_n \right) \right], \tag{86}$$

$$Y_4 = \frac{\beta E_g N_0 L_n}{4k |1-(\beta L_n)^2| a_t} \times \left(2 \coth \frac{d}{L_n} + \operatorname{csch} \frac{d}{L_n} - \beta L_n \right). \tag{87}$$

In the optically opaque situation $\beta L_n \gg 1$, Eqs. (86) and (87) combined yield

$$|\Delta T_G| \approx \frac{E_g N_0}{2\sqrt{2} k \beta L_n a_t(\omega)} \left| 2 \coth \frac{d}{L_n} + \operatorname{csch} \frac{d}{L_n} - \beta L_n \right|, \quad \Theta_{\Delta T} \approx -\pi/4. \tag{88}$$

In the fashion similar to the photocurrent signal amplitude $|J_G|$, $|\Delta T_G|$ is a function of β^{-1}, except for very high β, for which it saturates optically. As in the $v_s = 0$ case, the thermal generation nature of $|\Delta T_G|$ results in $f^{-1/2}$ (thermal-diffusion-length-controlled) dependence on modulation frequency.

2. High-frequency limit

The approximations described by Eqs. (44) and (45) are now valid and the minority-carrier ac diffusion length $\mu_j(\omega)$, Eq. (46), becomes a pertinent characteristic dimension of the problem.

(i) $v_s \to 0$:

Equations (47)–(53) are valid. In addition, the following approximations (Appendix B) can be made:

$$|Z_3| \approx 2|\mu_t^{-2} - \mu_n^{-2}| \equiv 2|a_t^2 - a_n^2|, \quad \phi_3 \approx \pi/2, \tag{89}$$

$$|Z_4| = \left[(\beta + a_t)^2 + a_t^2 \right]^{1/2} \approx \beta, \quad \phi_4 \approx 0. \tag{90}$$

Under the reasonable assumption $\beta^2 \gg (a_t + a_n) a_n$ in the optically opaque limit, Eq. (77) and its counterpart for Y_4 yield

$$X_4 \approx \frac{E_g N_0 \beta^2 D_n^{1/2}}{2k\tau_n \omega^{3/2}} \left[\frac{1}{2(a_t + a_n) a_t} \cos \left(\pi + \psi_2 - \frac{d}{\mu_n} \right) - \frac{(a_n/a_t)}{|a_t^2 - a_n^2|} e^{-(a_t + a_n)d} \cos(\pi + \psi_2 + a_t d) \right] \tag{91}$$

and

$$Y_4 \approx -\frac{E_g N_0 \beta^2 D_n^{1/2}}{2k\tau_n \omega^{3/2}} \left[\frac{1}{2(a_t + a_n) a_t} \sin \left(\pi + \psi_2 - \frac{d}{\mu_n} \right) - \frac{(a_n/a_t)}{|a_t^2 - a_n^2|} e^{-(a_t + a_n)d} \sin(\pi + \psi_2 + a_t d) \right]. \tag{92}$$

Typically, $a_t(1\ \text{MHz}) \approx 1.72 \times 10^3\ \text{cm}^{-1}$ for crystalline Si,[4] and $a_n(1\ \text{MHz}) \approx 1.79 \times 10^3\ \text{cm}^{-1}$ for a p^+-type diffused layer in a Si-based p-n junction,[9] so that $(a_t + a_n) a_t \gg 1$. From the form of Eqs. (91) and (92), it is easy to see that

$$|a_t^2 - a_n^2| = |a_t - a_n|(a_t + a_n) \ll a_t (a_t + a_n). \tag{93}$$

Therefore, combining Eqs. (91)–(93) gives

$$|\Delta T_G| \approx \frac{E_g N_0 \beta^2 \alpha^{1/2}}{k\tau_n \omega^{3/2} |a_t^2 - a_n^2|} \exp[-(a_t + a_n)d], \quad (94)$$

$$\Theta_T(\omega) \approx \pi + \psi_2(\omega) + a_t(\omega)d. \quad (95)$$

The amplitude decays exponentially with an approximate slope of $[\sqrt{\pi}/(\sqrt{\alpha} + \sqrt{D_n})]d$ on a $\ln|\Delta T_G|$ vs $f^{1/2}$ plot. A preexponential frequency dependence on $\omega^{-5/2}$ is also predicted by Eq. (94). This dependence may be understood in terms of a combination of carrier diffusional and thermal wave attenuations as functions of modulation frequency: the ω^{-1} decrease due to the photogenerated plasma wave contribution, Eq. (54), is combined with the $\omega^{-3/2}$ decrease due to high-frequency thermal wave attenuation, a well-known photothermal wave behavior in semiconductors in the optically opaque and thermally thick limit.[15]

(ii) $v_s \to \infty$:

In this limit Eqs. (56)–(59) are valid. In addition, Eqs. (89) and (90) hold and the real and imaginary signal components can be written:

$$X_4 \approx \frac{E_g N_0 \beta}{2k\tau_n \omega} \left(\frac{1}{2(a_t + a_n)a_t} + \frac{(a_n/a_t)}{|a_t^2 - a_n^2|} e^{-(a_t + a_n)d} \times \cos[\pi + (a_t + a_n)d] + \frac{\beta L_n^2}{2a_t} \right) \quad (96)$$

and

$$Y_4 \approx \frac{E_g N_0 \beta}{2k\tau_n \omega} \left(\frac{(a_n/a_t)}{|a_t^2 - a_n^2|} e^{-(a_t + a_n)d} \sin[\pi + (a_t + a_n)d] + \frac{L_n^2}{2a_t}(\beta + 2a_n) \right). \quad (97)$$

Using relation (93) as in case (i) above, and, for opaque semiconductors, $L_n^2 \ll 1/\beta\,[a_t(\omega) + a_n(\omega)]$, Eqs. (96) and (97) may be combined yielding

$$|\Delta T_G| \approx \frac{E_g N_0 \beta (\alpha/D_n)^{1/2}}{k\tau_n \omega |a_t^2 - a_n^2|} \exp[-(a_t + a_n)d], \quad (98)$$

$$\Theta_T(\omega) \approx \pi + [a_t(\omega) + a_n(\omega)]d. \quad (99)$$

The ac PTR amplitude exhibits a ω^{-2} preexponential dependence and an exponential decay with $f^{1/2}$ identical to that of Eq. (94) valid in the limit $v_s = 0$. This behavior may also be understood as a combination of the $\omega^{-1/2}$ decrease due to the photogenerated plasma wave contribution, Eq. (60) and the $\omega^{-3/2}$ thermal wave attenuation in the semiconductor in the optically opaque and thermally thick limit.[15] It is interesting to notice that the preexponential frequency-dependence difference between the PTR $v_s \to 0$ and $v_s \to \infty$ cases is a $\omega^{-1/2}$ factor. This is the same difference as the one observed between the photocurrent signals under the same conditions, Eqs. (54) and (60). A direct comparison between the electronic transport parameter information content of the high-frequency photocurrent and PTR analytical expressions derived in this work shows the following: In the $v_s \to 0$ limit, $|J_G|$ and $|\Delta T_G|$ both decay exponentially with $f^{1/2}$, however, the slopes are, respectively, $(\pi/D_n)^{1/2}d$ and $[\pi^{1/2}/(\alpha^{1/2} + D_n^{1/2})]d$. The preexponential factors are proportional to β^2, and $|J_G|$ depends on D_n, while $|\Delta T_G|$ has both D_n and τ_n dependencies due to the heat release mechanism following minority-carrier diffusion and recombination with a time constant τ_n. Of course, thermal wave diffusion information is exclusively present in $|\Delta T_G|$, manifesting itself as a different power dependence on f than $|J_G|$ and in the presence of the material thermal properties α, k, c. These observations demonstrate that similar electronic and optical information about the p-n junction device can be obtained from either photocurrent or PTR data in the $v_s \to 0$ limit, with a combination of the two techniques yielding the optimum number of parameter measurements. In the $v_s \to \infty$ limit, entirely analogous comments can be made, with both techniques depending on β linearly (optically opaque limit) and ac PTR exhibiting a τ_n dependence, as well as the (common) D_n dependence.

IV. CONCLUSIONS

The coupled ac photocurrent and PTR theories presented in this work show that electronic transport information can be obtained using a laser-induced PTR signal in a p-n junction photovoltaic device, such as a solar cell. The ac thermoreflectance signal frequency dependence was shown to be sensitive to D_n, τ_n, and d parameters. Therefore, the present theory sets the foundation for the utilization of ac PTR as a noncontact electronic property diagnostic measurement technique at the device level. In principle, optimum diagnostic ability was found to exist when both PTR and photocurrent measurements take place simultaneously.

APPENDIX A

Polar form representation of complex functions in ac photovoltaic theory

The basic building-block complex-valued functions appearing in Eq. (28) can be written in the form $|Q|e^{i\phi}$ as follows:

$$L_{\omega j} = (L_j/|R_j|^{1/2})e^{i\phi_j/2}, \quad (A1)$$

where

$$L_j(D_j\tau_j)^{1/2}, \quad |R_j| = [1 + (\omega\tau_j)^2]^{1/2},$$
$$\phi_j = \tan^{-1}(\omega\tau_j), \quad j \equiv n \text{ or } p.$$

$$\cosh(d/L_{\omega n}) = |Z_c|e^{i\phi_c}, \quad (A2)$$

where

$$|Z_c| = [\sinh^2(C_n) + \cos^2(S_n)]^{1/2},$$
$$\phi_c = \tan^{-1}[\tan(S_n)\tanh(C_n)],$$

with

$$C_n = (d|R_n|^{1/2}/L_n)\cos(\phi_n/2) \quad (A3)$$

and

$$S_n = (d|R_n|^{1/2}/L_n)\sin(\phi_n/2). \quad (A4)$$

$$\sinh(d/L_{\omega n}) = |Z_s|e^{i\phi_s}, \quad (A5)$$

where

$$|Z_s| = [\sinh^2(C_n) + \sin^2(S_n)]^{1/2}$$

and

$$\phi_s = \tan^{-1}[\tan(S_n)\coth(C_n)].$$

$$1 - \beta^2 L_{\omega n}^2 = |Z_1| e^{i\phi_1}, \tag{A6}$$

where

$$|Z_1| = \{[1 - (\beta^2 L_n^2/|R_n|)\cos\phi_n]^2 + (\beta^2 L_n^2/|R_n|)^2 \sin^2\phi_n\}^{1/2},$$

$$\phi_1 = \tan^{-1}\left(\frac{(\beta^2 L_n^2/|R_n|)\sin\phi_n}{1 - (\beta^2 L_n^2/|R_n|)\cos\phi_n}\right).$$

$$1 - \beta^2 L_{\omega p}^2 = |Z_2| e^{i\phi_2}, \tag{A7}$$

where

$$|Z_2| = \{[1 - (\beta^2 L_p^2/|R_p|)\cos\phi_p]^2 + (\beta^2 L_p^2/|R_p|)^2 \sin^2\phi_p\}^{1/2},$$

$$\phi_2 = \tan^{-1}\left(\frac{(\beta^2 L_p^2/|R_p|)\sin\phi_p}{1 - (\beta^2 L_p^2/|R_p|)\cos\phi_p}\right).$$

Finally, the complex functions that make up Eq. (28) may be constructed from the above basic functions upon defining

$$J_1 = X_1 + iY_1 \equiv |J_1| e^{i\Psi_1}, \tag{A8}$$

$$J_2 = X_2 + iY_2 \equiv |J_2| e^{i\Psi_2}, \tag{A9}$$

where

$$J_1 \equiv v_s \cosh(d/L_{\omega n}) + (D_n/L_{\omega n})\sinh(d/L_{\omega n}), \tag{A10}$$

$$X_1 = v_s \cosh(C_n)\cos(S_n) + (D_n|R_n|^{1/2}/L_n) \times [\cos(\phi_n/2)\cos(S_n)\sinh(C_n) - \sin(\phi_n/2) \times \sin(S_n)\cosh(C_n)]. \tag{A11}$$

and

$$Y_1 = v_s \sinh(C_n)\sin(S_n) + (D_n|R_n|^{1/2}/L_n) \times [\sin(\phi_n/2)\cos(S_n)\sinh(C_n) + \cos(\phi_n/2) \times \sin(S_n)\cosh(C_n)]. \tag{A12}$$

The complex function J_2 is defined as

$$J_2 \equiv (D_n/L_{\omega n})\cosh(d/L_{\omega n}) + v_s \sinh(d/L_{\omega n}), \tag{A13}$$

with

$$X_2 = v_s \sinh(C_n)\cos(S_n) + (D_n|R_n|^{1/2}/L_n) \times [\cos(\phi_n/2)\cos(S_n)\cosh(C_n) - \sin(\phi_n/2) \times \sin(S_n)\sinh(C_n)]$$

and

$$Y_2 = v_s \cosh(C_n)\sin(S_n) + (D_n|R_n|^{1/2}/L_n) \times [\sin(\phi_n/2)\cos(S_n)\cosh(C_n) + \cos(\phi_n/2) \times \sin(S_n)\sinh(C_n)].$$

In Eqs. (A8) and (A9) amplitudes and phases are given by

$$|J_k| = (X_k^2 + Y_k^2)^{1/2}, \tag{A14}$$

$$\psi_k = \tan^{-1}(Y_k/X_k), \quad k = 1,2. \tag{A15}$$

Now the amplitude $|J_G|$ and phase Θ_G of the photocurrent signal can be written as

$$|J_G| = (X_3^2 + Y_3^2)^{1/2}, \tag{A16}$$

$$\Theta_G = \tan^{-1}(Y_3/X_3), \tag{A17}$$

where

$$X_3 = \frac{1}{2} q\beta N_0 \left(\frac{L_p}{|R_p|^{1/2}|Z_2|}\left[\cos\left(\phi_2 + \frac{\phi_p}{2}\right) - \frac{\beta L_p}{|R_p|^{1/2}}\cos(\phi_2 + \phi_p)\right] e^{-\beta d} + \frac{L_n}{|R_n|^{1/2}|Z_1|}\left\{\left[\frac{|J_1|}{|J_2|}\cos\left(\psi_1 - \psi_2 - \phi_1 - \frac{\phi_n}{2}\right) + \frac{\beta L_n}{|R_n|^{1/2}}\cos(\phi_1 + \phi_n)\right] e^{-\beta d} - \frac{v_s + \beta D_n}{|J_2|}\cos\left(\psi_2 + \phi_1 + \frac{\phi_n}{2}\right)\right\}\right) \tag{A18}$$

and

$$Y_3 = \frac{1}{2} q\beta N_0 \left(\frac{L_p}{|R_p|^{1/2}|Z_2|}\left(\frac{\beta L_p}{|R_p|^{1/2}}\sin(\phi_2 + \phi_p)\right) - \sin\left(\phi_2 + \frac{\phi_p}{2}\right) e^{-\beta d} + \frac{L_n}{|R_n|^{1/2}|Z_1|}\left\{\left[\frac{|J_1|}{|J_2|}\sin\left(\psi_1 - \psi_2 - \phi_1 - \frac{\phi_n}{2}\right) - \frac{\beta L_n}{|R_n|^{1/2}}\sin(\phi_1 + \phi_n)\right] e^{-\beta d} + \frac{v_s + \beta D_n}{|J_2|}\sin\left(\psi_2 + \phi_1 + \frac{\phi_n}{2}\right)\right\}\right). \tag{A19}$$

APPENDIX B

Polar form representation of complex functions in ac PTR theory

In addition to functions presented in appendix A, Eq. (76) requires the polar transformation of several thermal-wave-related expressions:

$$\sigma = (i\omega/\alpha)^{1/2} = (1+i)(\omega/2\alpha)^{1/2} \equiv \sqrt{2}a_t e^{i\pi/4}, \quad \text{(B1)}$$

where $a_t \equiv (\omega/2\alpha)^{1/2}$ is the thermal diffusion coefficient. Sometimes it is convenient to define a thermal diffusion length $\mu_t(\omega) \equiv 1/a_t(\omega) = (2\alpha/\omega)^{1/2}$,

$$\sigma^2 - L_{\omega n}^{-2} = |Z_3| e^{i\phi_3}, \quad \text{(B2)}$$

where

$$|Z_3| = \{[2a_t^2 - (|R_n|/L_n^2)\sin\phi_n]^2 + (|R_n|/L_n^2)^2\cos^2\phi_n\}^{1/2},$$

$$\phi_3 = \tan^{-1}\left(\frac{2a_t^2 - (|R_n|/L_n^2)\sin\phi_n}{-(|R_n|/L_n^2)\cos\phi_n}\right).$$

$$\sigma + \beta = |Z_4| e^{i\phi_4} \quad \text{(B3)}$$

where

$$|Z_4| = [(\beta + a_t)^2 + a_t^2]^{1/2},$$

$$\phi_4 = \tan^{-1}[a_t/(a_t+\beta)].$$

$$1 - (\sigma L_{\omega n})^{-2} = |Z_5| e^{i\phi_5}, \quad \text{(B4)}$$

where

$$|Z_5| = \{[1 - (|R_n|/2a_t^2 L_n^2)\sin\phi_n]^2 + (|R_n|/2a_t^2 L_n^2)^2\cos^2\phi_n\}^{1/2},$$

$$\phi_5 = \tan^{-1}\left(\frac{(|R_n|/2a_t^2 L_n^2)\cos\phi_n}{1 - (|R_n|/2a_t^2 L_n^2)\sin\phi_n}\right).$$

$$\sigma + L_{\omega p}^{-1} = |Z_6| e^{i\phi_6}, \quad \text{(B5)}$$

where

$$|Z_6| = \{[a_t(|R_p|^{1/2}/L_p)\cos(\phi_p/2)]^2 + [a_t + (|R_p|^{1/2}/L_p)\sin(\phi_p/2)]^2\}^{1/2},$$

$$\phi_6 = \tan^{-1}\left(\frac{a_t + (|R_p|^{1/2}/L_p)\sin(\phi_p/2)}{a_t + (|R_p|^{1/2}/L_p)\cos(\phi_p/2)}\right).$$

Using functional definitions from Appendixes A and B, the amplitude $|\Delta T_G|$ and phase $\Theta_{\Delta T}$ of the PTR signal, from Eq. (76), can be written in the form

$$|\Delta T_G| = (X_4^2 + Y_4^2)^{1/2}, \quad \text{(B6)}$$

$$\Theta_{\Delta T} = \tan^{-1}(Y_4/X_4), \quad \text{(B7)}$$

where

$$\begin{aligned}
X_4 = &-\frac{\beta E_g N_0}{2k}\left[\frac{1}{\sqrt{2}a_t|R_p||Z_2|}\left[\frac{1}{|Z_6|}\cos\left(\phi_p+\phi_2+\phi_6+a_t d+\frac{\pi}{4}\right)\right.\right.\\
&\left.-\frac{1}{|Z_4|}\cos\left(\phi_p+\phi_2+\phi_4+a_t d+\frac{\pi}{4}\right)\right]e^{-(\beta+a_t)d}+\frac{1}{|R_n||Z_1|}\\
&\times\left(\frac{1}{|J_2|}\left(\frac{1}{|Z_3|}\left(\frac{D_n|R_n|^{1/2}}{L_n}e^{-\beta d}\cos\left(\frac{\phi_n}{2}+\phi_1+\phi_3+\psi_2\right)+(v_s+\beta D_n)|Z_s|\cos(\phi_n+\phi_1+\phi_3+\psi_2-\phi_s)\right)\right.\right.\\
&+\frac{|R_n|^{1/2}}{\sqrt{2}a_t L_n}\left\{v_s e^{-\beta d}\cos\left(\frac{\phi_n}{2}+\phi_1+\phi_3+\psi_2+\frac{\pi}{4}\right)-(v_s+\beta D_n)\left[|Z_c|\cos\left(\frac{\phi_n}{2}+\phi_1+\phi_3+\psi_2+\frac{\pi}{4}-\phi_c\right)\right.\right.\\
&\left.\left.+e^{-\beta d}\cos\left(\frac{\phi_n}{2}+\phi_1+\phi_3+\psi_2+a_t d+\frac{\pi}{4}\right)\right]-|J_1|e^{-(\beta+a_t)d}\cos\left(\frac{\phi_n}{2}+\phi_1+\phi_3+\psi_2+a_t d+\frac{\pi}{4}-\psi_1\right)\right\}\Bigg)\\
&+\frac{v_s\tau_n}{\sqrt{2}a_t}\left\{\frac{D_n|R_n|^{1/2}}{L_n}\left[e^{-\beta d}\cos\left(\frac{\phi_n}{2}+\phi_1+\psi_2+\frac{\pi}{4}\right)-|Z_c|\cos\left(\frac{\phi_n}{2}+\phi_1+\psi_2+\frac{\pi}{4}-\phi_c\right)\right]\right.\\
&\left.\left.+\beta D_n|Z_s|\cos\left(\phi_n+\phi_1+\psi_2+\frac{\pi}{4}-\phi_s\right)\right\}\right)-\frac{1}{\sqrt{2}a_t}\left\{\frac{1}{|Z_4|}\cos\left(\phi_n+\phi_1+\phi_4+\frac{\pi}{4}\right)\right.\\
&\left.\left.-\left[\frac{1}{|Z_4|}\cos\left(\phi_n+\phi_1+\phi_4+a_t d+\frac{\pi}{4}\right)-\frac{1}{\sqrt{2}a_t|Z_5|}\cos\left(\phi_n+\phi_1+\phi_5+a_t d+\frac{\pi}{2}\right)\right]e^{-(\beta+a_t)d}\right\}\right]. \quad \text{(B8)}
\end{aligned}$$

Similarly,

$$\begin{aligned}
Y_4 = &\frac{\beta E_g N_0}{2k}\left[\frac{1}{\sqrt{2}a_t|R_p||Z_2|}\left[\frac{1}{|Z_6|}\sin\left(\phi_p+\phi_2+\phi_6+a_t d+\frac{\pi}{4}\right)\right.\right.\\
&\left.\left.-\frac{1}{|Z_4|}\sin\left(\phi_p+\phi_2+\phi_4+a_t d+\frac{\pi}{4}\right)\right]e^{-(\beta+a_t)d}+\frac{1}{|R_n||Z_1|}\right.
\end{aligned}$$

$$\times\left(\frac{1}{|J_2|}\left(\frac{1}{|Z_3|}\left(\frac{D_n|R_n|^{1/2}}{L_n}e^{-\beta d}\sin\left(\frac{\phi_n}{2}+\phi_1+\phi_3+\psi_2\right)+(v_s+\beta D_n)|Z_s|\sin(\phi_n+\phi_1+\phi_3+\psi_2-\phi_s)\right.\right.\right.$$
$$+\frac{|R_n|^{1/2}}{\sqrt{2}a_tL_n}\left\{v_se^{-\beta d}\sin\left(\frac{\phi_n}{2}+\phi_1+\phi_3+\psi_2+\frac{\pi}{4}\right)-(v_s+\beta D_n)\left[|Z_c|\sin\left(\frac{\phi_n}{2}+\phi_1+\phi_3+\psi_2+\frac{\pi}{4}-\phi_c\right)\right.\right.$$
$$\left.\left.+e^{-\beta d}\sin\left(\frac{\phi_n}{2}+\phi_1+\phi_3+\psi_2+a_td+\frac{\pi}{4}\right)\right]-|J_1|e^{-(\beta+a_t)d}\sin\left(\frac{\phi_n}{2}+\phi_1+\phi_3+\psi_2+a_td+\frac{\pi}{4}-\psi_1\right)\right\}\Bigg)$$
$$+\frac{v_s\tau_n}{\sqrt{2}a_t}\left\{\frac{D_n|R_n|^{1/2}}{L_n}\left[e^{-\beta d}\sin\left(\frac{\phi_n}{2}+\phi_1+\psi_2+\frac{\pi}{4}\right)-|Z_c|\sin\left(\frac{\phi_n}{2}+\phi_1+\psi_2+\frac{\pi}{4}-\phi_c\right)\right]\right.$$
$$\left.+\beta D_n|Z_s|\sin\left(\phi_n+\phi_1+\psi_2+\frac{\pi}{4}-\phi_s\right)\right\}\Bigg)-\frac{1}{\sqrt{2}a_t}\left\{\frac{1}{|Z_4|}\sin\left(\phi_n+\phi_1+\phi_4+\frac{\pi}{4}\right)\right.$$
$$\left.-\left[\frac{1}{|Z_4|}\sin\left(\phi_n+\phi_1+\phi_4+a_td+\frac{\pi}{4}\right)-\frac{1}{\sqrt{2}a_t|Z_5|}\sin\left(\phi_n+\phi_1+\phi_5+a_td+\frac{\pi}{2}\right)\right]e^{-(\beta+a_t)d}\right\}\Bigg)\Bigg]. \quad \text{(B9)}$$

[1] J. P. McKelvey, *Solid State and Semiconductor Physics* (Harper and Row, New York, 1966), Chap. 13.6.
[2] C. Munakata, K. Yagi, T. Warabisako, M. Nanba, and S. Matsubara, Jpn. J. Appl. Phys. **21**, 624 (1982).
[3] N. Honma, C. Munakata, H. Itoh, and T. Warabisako, Jpn. J. Appl. Phys. **25**, 743 (1986).
[4] A. Rosencwaig, in *Photoacoustic and Thermal Wave Phenomena in Semiconductors*, edited by A. Mandelis (North-Holland, New York, 1987), Chap. 5.
[5] W. L. Smith, A. Rosencwaig, and D. L. Willenborg, Appl. Phys. Lett. **47**, 584 (1985).
[6] J. Opsal and A. Rosencwaig, Appl. Phys. Lett. **47**, 498 (1985).
[7] A. Mandelis, A. Williams, and E. K. M. Siu, J. Appl. Phys. **63**, 92 (1988).
[8] A. Mandelis, A. A. Ward, and K. T. Lee, J. Appl. Phys. **66**, 5584 (1989).
[9] A. L. Fahrenbruch and R. H. Bube, *Fundamentals of Solar Cells* (Academic, New York, 1983), Chap. 7.4.
[10] J. P. McKelvey, *Solid State and Semiconductor Physics* (Harper and Row, New York, 1966), Chap. 15.1.
[11] C. Munakata, N. Honma, and H. Itoh, Jpn. J. Appl. Phys. **22**, L103 (1983).
[12] B. Batz, in *Semiconductors and Semimetals*, edited by R. K. Willardson and A. C. Beer (Academic, New York, 1972), Chap. 4.
[13] H. A. Weaklim and D. Redfield, J. Appl. Phys. **50**, 1491 (1979).
[14] J. R. Meyer, F. J. Bartoli, and M. R. Kruer, Phys. Rev. B **21**, 1559 (1980).
[15] A. Rosencwaig, Rev. Sci. Instrum. **48**, 1133 (1977).